Nanosized Cs-pollucite zeolite synthesized under mild condition and its catalytic behavior

Aleid Ghadah Mohammad S, Nur Hidayahni Ahmad, Kamila Goldyn, Svetlana Mintova, Tau Chuan Ling, Eng-Poh Ng

Nanosized Cs-Pollucite Zeolite Synthesized under Mild Condition and Its Catalytic Behavior

Ghadah Aleid,[a,b] Nurhidayahni Ahmad,[a] Kamila Goldyn,[c] Svetlana Mintova,[c] Tau Chuan Ling,[d] Eng-Poh Ng[a,*]

[a]*School of Chemical Sciences, Universiti Sains Malaysia, 11800 USM, Penang, Malaysia.*

[b]*Department of Chemistry (Preparatory Year), Faculty of Science, University of Hail, P.O. Box 2440, Hail, Kingdom of Saudi Arabia.*

[c]*Laboratoire Catalyse & Spectrochimie, ENSICAEN, Université de Caen, 14000 Caen, France.*

[d]*Institute of Biological Sciences, Faculty of Science, University of Malaya, 50603 Kuala Lumpur, Malaysia.*

**Corresponding author. E-mail address: epng@usm.my*

Abstract

Nanoscale cesium-pollucite zeolite (ANA topology) free of organic template is synthesized free of organic template. The crystallization is taken place at mild temperature and pressure (180 °C, 22 bar) compared to previous works. Powder XRD analysis reveals that the nanocrystals can be crystallized from a clear precursor solution of $16.5SiO_2$:$1Al_2O_3$:$5.3Cs_2O$:$175H_2O$ within 50 h. The resulting nanocrystals exhibit trapezohedron shape and has a Si/Al ratio of 4.11. The nanocrystals possess a mean particle size of 79.4 nm and they are colloidally stable in water. In addition, Perkin condensation of benzaldehyde with acetic anhydride catalyzed by nanosized Cs-pollucite zeolite under non-microwave instant heating condition is also demonstrated and discussed.

Keywords: Nanocrystals; Cesium-pollucite; Template-free synthesis; Mild synthesis condition; Perkin Condensation

1. Introduction

Nanoscale science and engineering provide unique understanding and control of matter and mostly on a fundamental level [1–3]. In particular, zeolite particles have been fascinating the world of science during the last two decades due to the uniform pore size and high surface area contributed by their crystalline pores and channels of molecular dimensions [4–6]. As a result, zeolites have been widely used in heterogeneous catalysis, ion-exchange and adsorption [7-9].

In recent years, scaling down the particle size of zeolites to nanometer range has become a hot topic since it creates substantial and new modification to the properties of the materials (e.g. external surface area, diffusivity, colloidal stability, electronic, etc.) that required for advanced applications such as in atomic energy production, electronics, recording materials, drug delivery, food, ceramics, paints, paper, detergents, lubricants and so on [8–11]. While more than 230 types of zeolites have been discovered today, only 17 types of nanocrystalline zeolites (*BEA [12], EDI [13], EMT [9], FAU [14, 15], GIS [16], LTA [17], LTJ [18], LTL [19], MEL [20], MER [21], MFI [22], MOR [23], SOD [24], AEI [25], AFI [26], AFO [27], CHA [28]) have been synthesized so far.

Cs-pollucite zeolite, $CsAlSi_2O_6$, which has 8-membered ring (pore diameter 2.43Å) and three-dimensional channel, is a very interesting material because of its Cs^+ extraframework cations that is highly aprreciated in solid basic-catalyzed organic reactions [29]. In addition, pollucite is also an excellent host for immobilization of radioactive cesium [30]. Typically, pollucite is crystallized at very high temperature and pressure (700-1200 °C, >1000 bar) by using solid state

reaction [31]. Hence, the synthesis of Cs-pollucite is rarely reported due to its tedious and extreme synthesis condition. Furthermore, the Cs with very high basicity tends to evaporate at such high temperature and it readily corrodes the reactors.

Recently, Cs-pollucite has been successfully crystallized under hydrothermal condition from zeolite or clay (300 °C, 850 bar) [32] and soil (200 °C, 300 bar) [33] at much lower temperature and pressure. However, the synthesis condition is still not ideal considering its high heating pressure and temperature. In addition, the resulting crystals are very big (> 2 μm). In order to reduce the crystallite size to nanometer realm, large excessive of harmful and expensive organic template might need to be added to control the nucleation over the crystal growth [34].

Mild and safer condition for the synthesis of Cs-pollucite (particularly for nanometer-sized crystals) with lower crystallization temperature and pressure still remain a challenge, and hence it is our intention to synthesize nanosized Cs-pollucite free of organic template using lower temperature and pressure. In addition, the catalytic behavior of nanosized Cs-pollucite zeolite will also be investigated in Perkin condensation of benzaldehyde with acetic anhydride under non-microwave instant heating.

2. Experimental

2.1. Synthesis of Cs-pollucite zeolite nanocrystals

Cs-pollucite zeolite nanocrystals were synthesized from a clear precursor with a molar composition of $16.5SiO_2$:$1Al_2O_3$:$5.3Cs_2O$:$175H_2O$. A clear aluminate solution was initially prepared by dissolving $CsOH.H_2O$ (10.500 g, Sigma-Aldrich) and $Al(OH)_3$ (1.242 g, Acros) in distilled water (8.063 g) at 105 °C for 18 h (300 rpm stirring). A clear silicate solution was prepared by mixing and stirring HS-40 (19.74 g, Sigma-Aldrich) and $CsOH.H_2O$ (3.70 g) in distilled water

(3.70 g) at room temperature for 10 min. Both solutions were then mixed under vigorous stirring (15 min, 500 rpm) before the resulting clear precursor solution was autoclaved for crystallization (180 °C). The resulting colloidal solid products were centrifuged (10000 rpm, 10 min) and washed with distilled water until pH 7 before freeze-drying.

2.2. Characterization

The crystallinity and purity of samples were analyzed by a PANalytical X'Pert PRO XRD diffractometer (CuK_α radiation, λ = 1.5406 Å, scan speed of 0.2°/min, step size of 0.02°). FESEM and TEM micrographs were obtained with Leo Supra 50VP and Philips CM-12 electron microscopes operated at 20 kV and 200 kV, respectively. The chemical composition of solid was determined by using a Philips PW2404 X-ray fluorescence (XRF) spectrometer. The infrared (IR) spectrum of the solid was recorded with a Perkin Elmer's System 2000 spectrometer using KBr pellet technique (KBr:sample ratio = 50:1). The porosity analysis was performed using a Micromeritics ASAP 2010 nitrogen adsorption analyzer. The sample was first degassed at 300 °C for 14 h prior to sorption at –196 °C. The detection and measurement of strength of basic sites was investigated using temperature-programmed desorption of carbon dioxide (CO_2-TPD). The analysis was performed on a BELCAT-B instrument where the sample (ca. 80 mg) was first degassed at 400 °C overnight. The sample was then adsorbed with CO_2 gas before the gas was slowly desorbed in the temperature range of 40 to 800 °C at a heating rate of 10 °C/min.

2.3. Catalytic Perkin condensation reaction under non-microwave instant heating condition

Nanosized Cs-pollucite zeolite (0.60 g or 0.13 mmol), benzaldehyde (1.0 mmol, 99%, Merck) and acetic anhydride (1.5 mmol, Merck) were added into a 10-mL quartz reaction vessel, capped and heated at 180–190 °C by using a Monowave 50 non-microwave instant heating reactor (Anton Paar). The reaction solution was isolated and analyzed with a GC-FID chromatograph (Agilent/HP 6890 GC, HP-5 capillary column) and the identity of the product was confirmed with a GC-MS spectrometer (Perkin-Elmer Clarus 500 system).

2.4. Catalyst reusability study

The nanosized Cs-pollucite zeolite, which was used after the first reaction run, was washed with diethyl ether (15 mL) for 5 times and air dried. The solid was re-activated again before it was used for the subsequent cycles of catalytic reaction using the same reaction condition. The solution after the reaction was withdrawn and separated from the zeolite catalyst before it was analyzed using a GC-FID.

3. Results and discussion

3.1. Preparation and characterization of Cs-pollucite zeolite nanocrystals

The pressure of in the autoclave is monitored during the crystallization process. The pressure raised progressively as the temperature increased. A maximum pressure of 22 bar was recorded and the pressure remained constant when the temperature reached 180 °C. As compared to previous works (700-1200 °C, >1000 bar [31]; 300 °C, 850 bar [32]; 200 °C, 300 bar [33], the temperature and pressure used for the synthesis of Cs-pollucite in our work are much lower thus allowing safer synthesis operation.

The evolutional formation of Cs-pollucite nanocrystals is studied using XRD technique. Initially the precursor is transparent and no solid is formed for the first 44 h. However, the solution is becoming more viscous. Hence, it indicates that polymerization of silicate and aluminate species is taking place [35]. At 47 h, further polymerization among precursor species leads to the formation of cloudy colloidal suspension. The sample after purified and dried was analyzed with XRD diffractometer and the sample is found to be an amorphous solid (Fig. 1a). Hence, further heating is needed to undergo induction process so that zeolite nuclei can be formed [36].

When the reaction is prolonged to 48 h, the XRD amorphous hump slowly disappears after 48 h (Fig. 1b). Several diffraction peaks start to appear at $2\theta = 24.3°$ [321], 26.1° [400], 30.7° [332] and 37.2° [440] revealing that Cs-pollucite zeolite nuclei has been formed in this sample [37]. The amorphous entity fully transforms into Cs-pollucite nanocrystals after 50 h of hydrothermal treatment (Fig. 1c). As shown, the XRD diffractogram shows the characteristic pattern of ANA phase and the pattern is similar to the pattern shown on ICDD card number 00-029-0407, PDF2 files [38]. The XRD peaks are broad indicating the small size of the Cs-pollucite nanocrystals. The size of the Cs-pollucite nanoparticles is calculated using the Scherrer equation and are found to be 72.3 nm. No crystalline competing phase is observed after 100 h of heating showing that Cs-pollucite structure is thermodynamically stable.

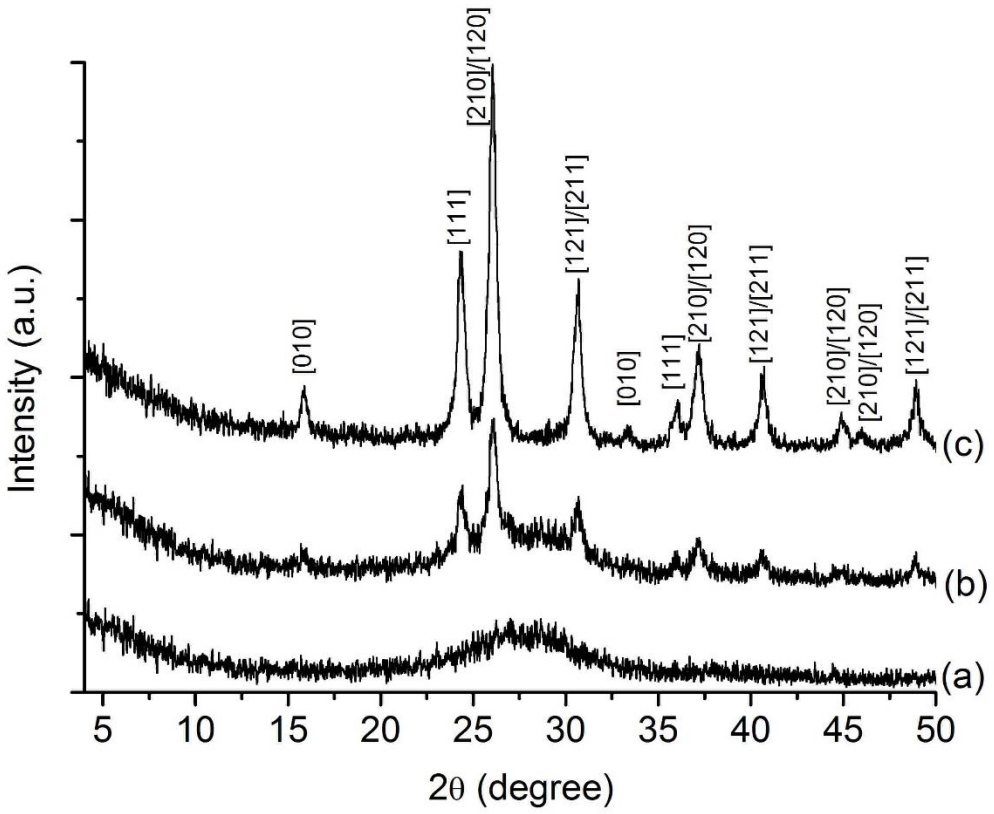

Fig. 1. XRD patterns of solids after (a) 47 h, (b) 48 h and (c) 50 h of hydrothermal synthesis.

The FESEM image of Cs-pollucite nanozeolite is captured and is shown in Fig. 2. It can be seen that the sample consists of discrete and non-agglomerated nanoparticles. The shape of the crystals is in spherical form but the crystal shape cannot be confirmed yet due to very small particle size of Cs-pollucite zeolite and low resolution of FESEM image. The particle size distribution of Cs-pollucite is determined by randomly counting the 100 crystals through FESEM observations obtained in different areas. Narrow monomodal particle size distribution centered at 79.4 nm with diameter ranging from 66.9 nm to 93.2 nm is shown indicating that the nanocrystals obtained have reasonably uniform crystal sizes (Fig. 2b).

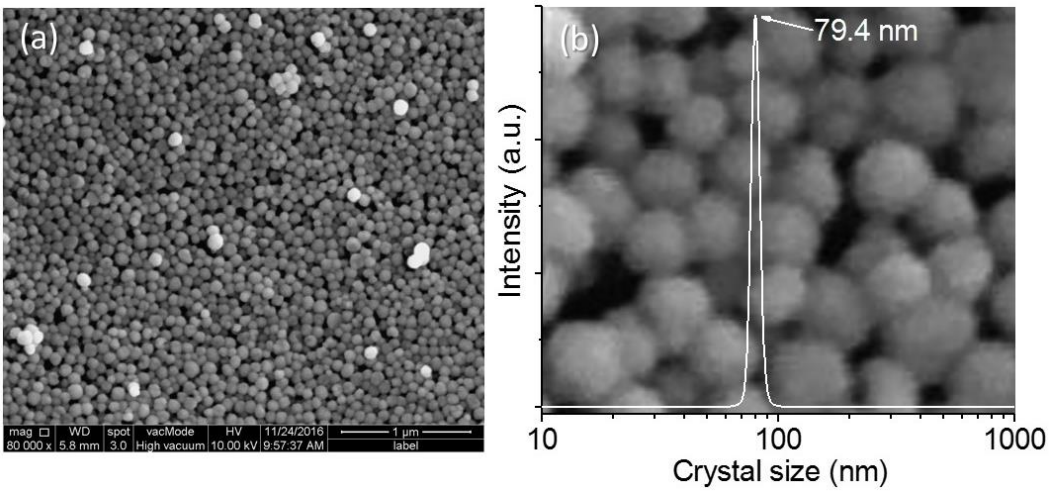

Fig. 2. (a,b) SEM images and (b) plot of particle size distribution of nanosized Cs-pollucite zeolite.

The morphology of nanocrystals are further characterized with TEM analysis. The TEM image shows that Cs-pollucite nanocrystals have a similar shape to the theoretical shape of ANA-type zeolite where its shape is trapezohedron with cubic symmetry (Fig. 3a). Similar crystal shape achieved by large pollucite crystal (40 μm) was also reported by Yokomori et al. where smectite and mordenite are used as aluminum and silicon sources [32]. Unlike micronsized zeolites, the nanosized Cs-pollucite can be easily dispersed in solvents like water (Fig. 3b). The suspension is colloidally stable at nominal size and no agglomeration of solid is observed for over 1 week. Hence, this colloidal stable Cs-pollucite can be potentially used in the advanced applications that require thin film deposition such as in sensors, ceramics, paints, electronics, recording materials, etc. [13, 39, 40].

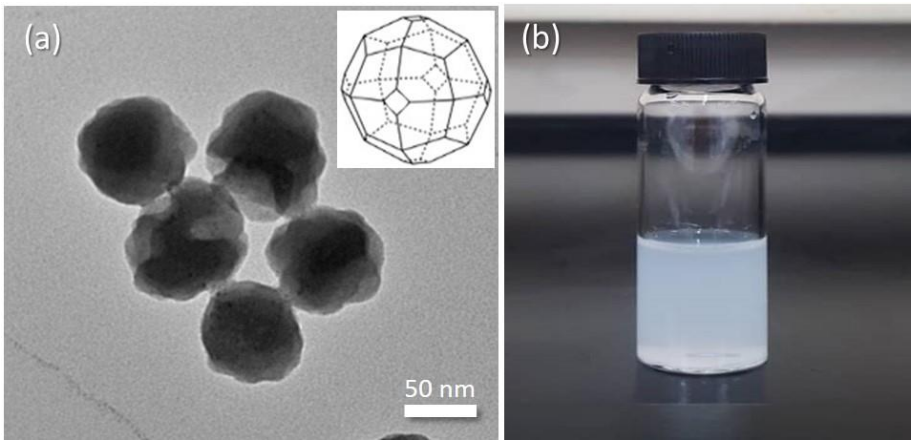

Fig. 3. (a) TEM image with theoretical shape (inset), and (b) colloidal solution of nanosized Cs-pollucite zeolite.

Complimentary IR spectroscopy study on the nanosized Cs-pollucite is also conducted and its IR spectrum is shown in Fig. 4a. The IR bands at 3458 and 1630 cm^{-1} are due to the stretching and bending modes of O–H groups of adsorbed water [41]. The strong band at 1035 cm^{-1} is assigned to the vibration frequency of the T–O–Si bonds (T = Si, Al) [42]. The IR bands at 774, 720 and 631 cm^{-1} are characteristic of highly distorted 8-rings subunits present in the pollucite zeolite [43]. Lastly, the IR vibration band at 441 cm^{-1} is ascribed to the bending vibration of TO_4 (T = Si, Al).

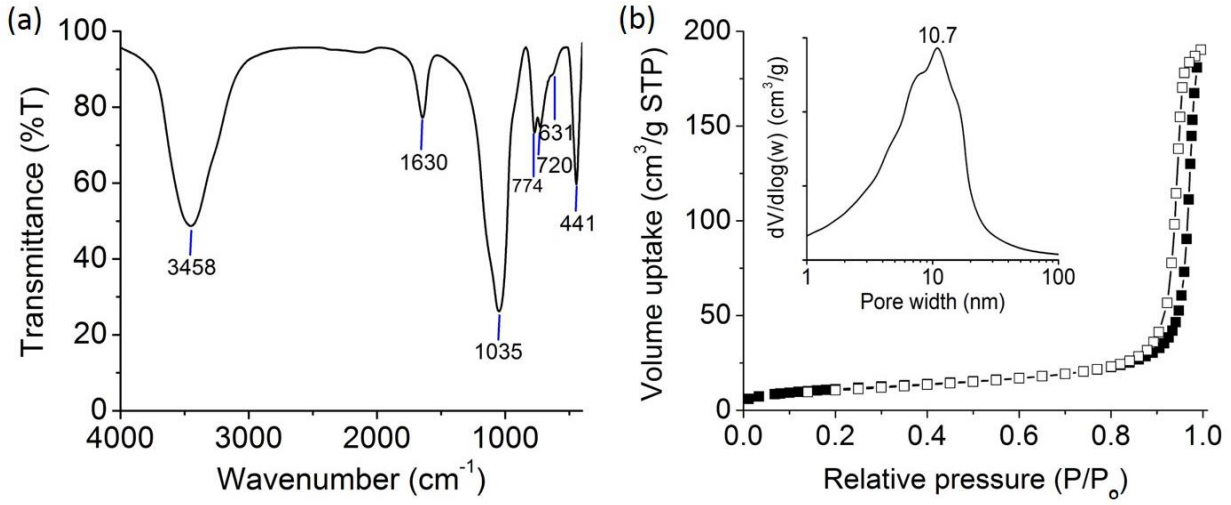

Fig. 4. (a) IR spectrum and (b) nitrogen adsorption (close symbol), desorption (open symbol) and pore size distribution (inset) of nanosized pollucite zeolite.

Nanocrystalline Cs-pollucite exhibits Type IV N_2 adsorption-desorption isotherm with H1 hysteresis loop (Fig. 4b). It indicates the presence of cylindrical or tubular type pores with a narrow distribution of mesopores of 10.7 nm due to the close-packing of nanocrystals [44]. Furthermore, an external surface area of 39 m^2/g and a total pore volume of 0.29 cm^3/g are also measured. No microporosity is detected due to the smaller pore size of pollucite zeolite ($\sigma = 2.43$ Å) than nitrogen probe molecules ($\sigma = 3.64$ Å) [45]. Nevertheless, this nanocrystalline material can be used as a catalyst since it contains highly basic Cs^+ extraframework cations on the external surface.

In order to confirm the presence of Cs element and to study the chemical composition in the Cs-pollucite nanozeolite, XRF spectroscopy analysis has been carried out. In general, the Si/Al ratio of Cs-pollucite zeolite is 2.0 while its theoretical molecular formula is $Cs_{16}[Al_{16}Si_{32}O_{96}]$ [43, 46]. Interestingly, the nanosized Cs-pollucite obtained in this work is a high-silica zeolite (Si/Al

ratio = 4.11) and the experimental molecular formula is calculated to be $Cs_{15.65}[Al_{7.78}Si_{32.00}O_{83.46}]$. Thus, the elemental analysis reveals that nanosized Cs-pollucite zeolite might have surface basicity.

The surface basicity of nanocrystalline Cs-pollucite is studied using CO_2-TPD analysis (Fig. 5). Three CO_2 desorption peaks are obtained after deconvolution of the TPD profile. The interaction of CO_2 with the weak basic sites located at the textural pores can be observed from the CO_2 desorption band at 88.1 °C. Meanwhile, the broad peak at 442 °C which can be deconvoluted into two peaks (442 °C and 603 °C) correspond to medium-to-strong basic sites located at the external surface of the zeolite.

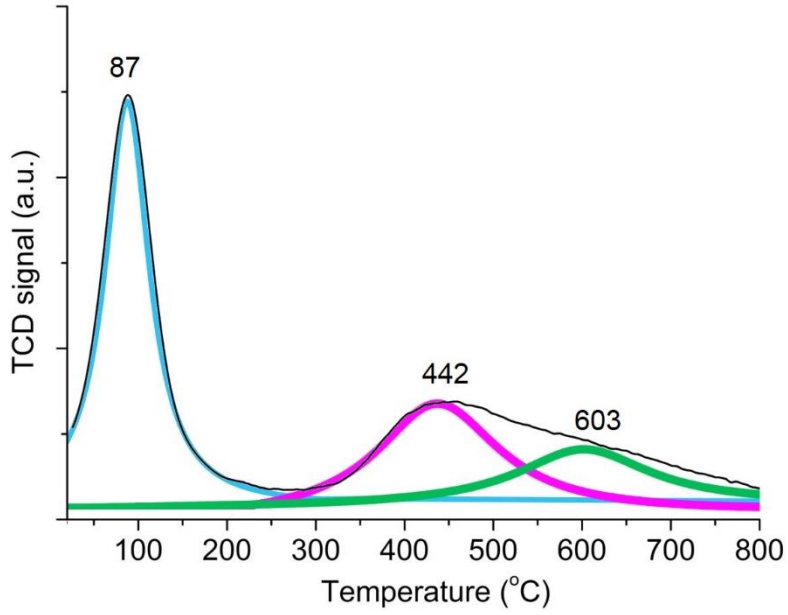

Fig. 5. CO_2-TPD profile of nanosized pollucite.

3.2. Catalytic reaction study

Perkin condensation of benzaldehyde with acetic anhydride is used as a model reaction to study the potential of Cs-pollucite nanozeolite as a solid base catalyst. The reaction produces only

cinnamic acid as sole product throughout the study (Scheme 1). As can be seen from Fig. 6, the conversion rate is low when no catalyst is added especially at 170 °C where only 29.4% of conversion is recorded after 80 min (Fig. 6a). When the reaction temperature is increased to 190 °C, the conversion increases to 65.1% using the same reaction time (Fig. 6c). On the other hand, the superior catalytic activity is shown by nanosized Cs-pollucite zeolite where high conversion (65.1%) is achieved at 170 °C. With further increasing the temperature to 190 °C, the highest conversion (92.2%) is recorded.

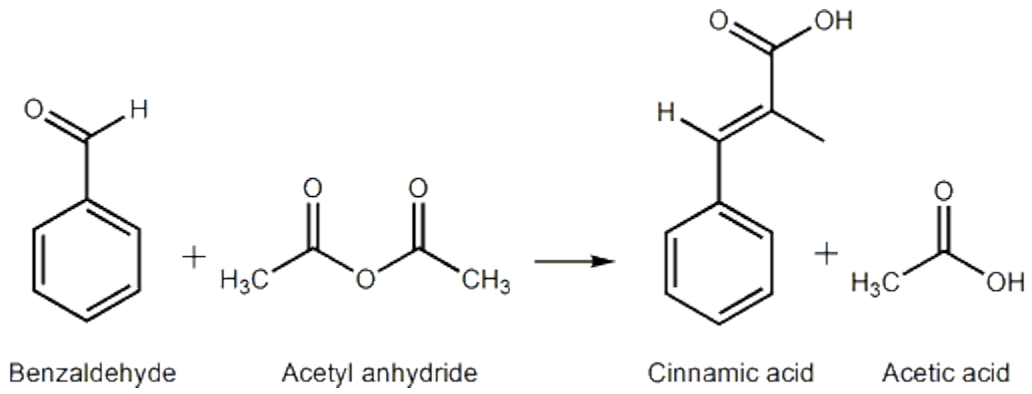

Scheme 1. Perkin condensation of benzaldehyde with acetyl anhydride to product cinnamic acid.

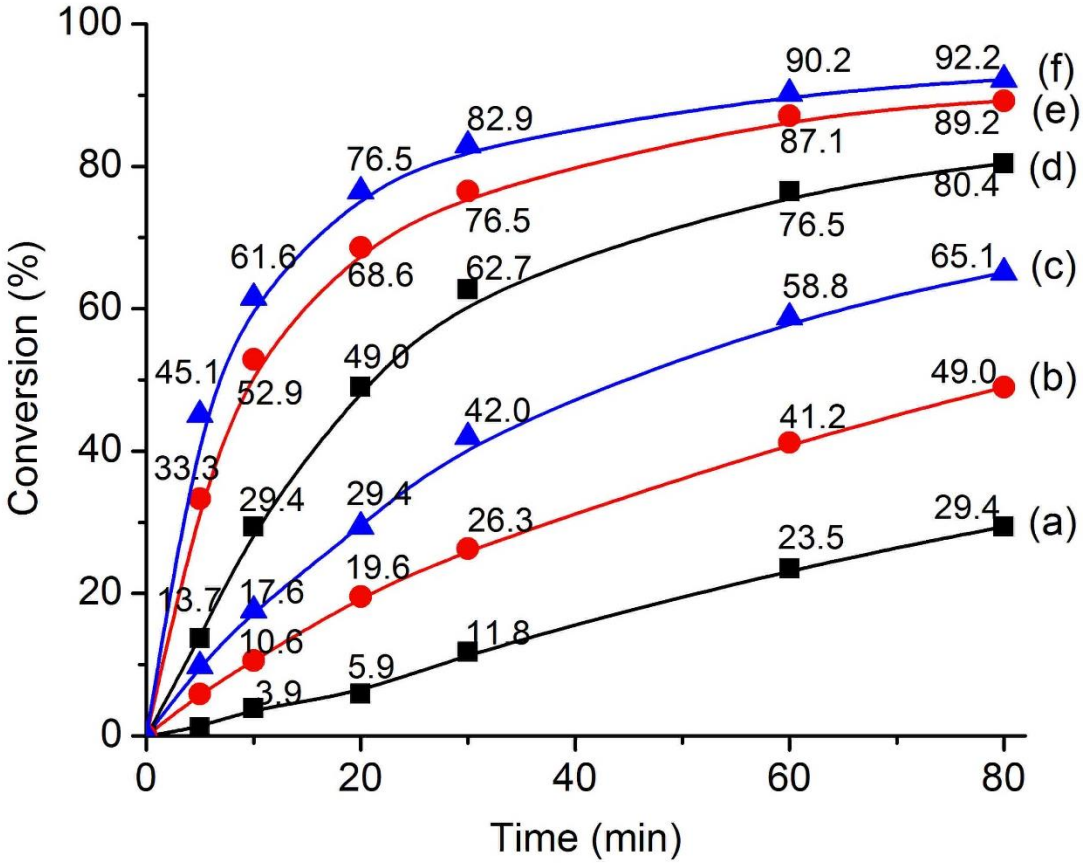

Fig. 6. Perkin condensation of benzaldehyde with acetic anhydride without catalyst at (a) 170 ºC, (b) 180 ºC and (c) 190 ºC, and with nanosized Cs-pollucite zeolite at (d) 170 ºC, (e) 180 ºC and (f) 190 ºC.

The results of reaction conversion over three different temperatures (170, 180 and 190 °C) are extracted to calculate the second order rate constants. The rate constants are then used to plot Arrhenius plots to determine the activation energy (E_a) of the reaction (Fig. 7). As calculated, the E_a of non-catalyzed Perkin condensation reaction is very high (144.89 kJ/mol). However, by adding nanosized Cs-pollucite zeolite as catalyst, the E_a is significantly reduced to 40.04 kJ/mol. Thus, this study shows that Perkin condensation of benzaldehyde is an activated catalytic reaction.

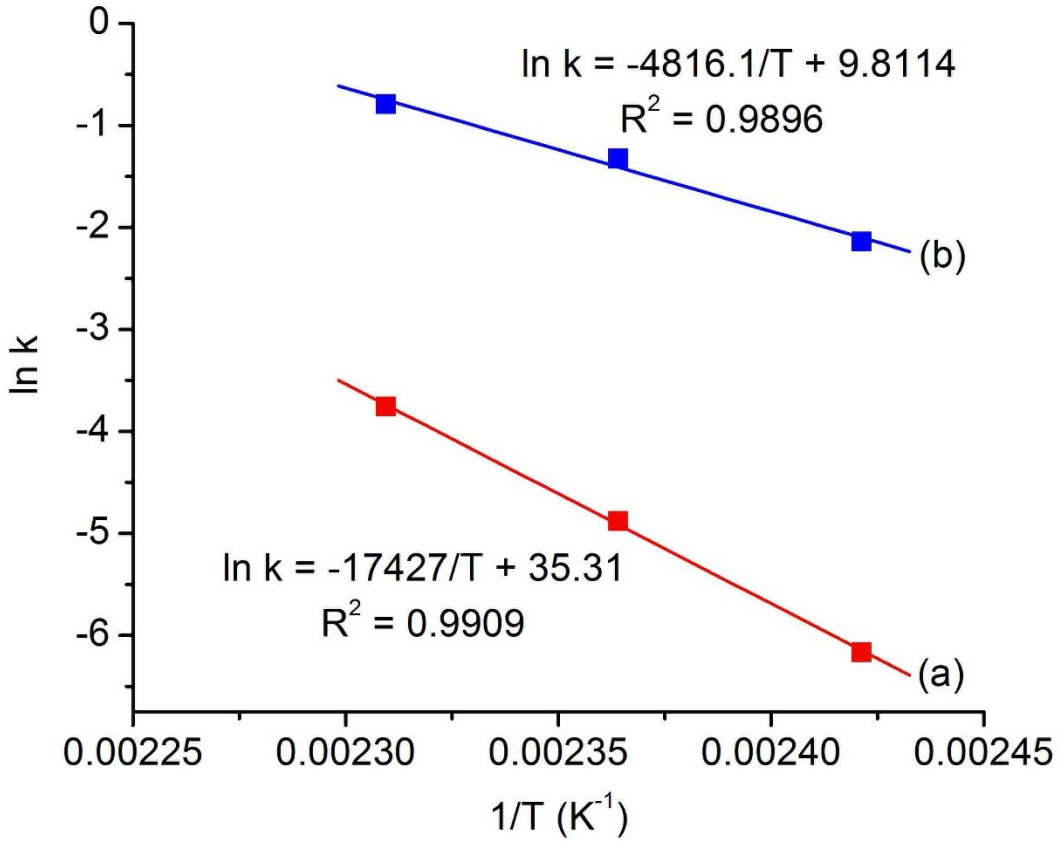

Fig. 7. Arrhenius plots of Perkin condensation of benzaldehyde performed (a) without catalyst and (b) with nanosized Cs-pollucite zeolite.

Comparative catalytic performance between nanosized Cs-pollucite zeolite and homogenous base catalysts such as sodium hydroxide and potassium hydroxide (equivalent molar amount to Cs-pollucite zeolite is added) is also performed at various reaction times (10, 20, 30 and 80 min) at 190 °C. As expected, potassium hydroxide gives higher conversion (90.1%) compared to sodium hydroxide (83.1%) after 80 min of reaction due to its high basicity (Fig. 8). On the other hand, nanosized Cs-pollucite zeolite performs slightly better than potassium hydroxide under the same reaction time.

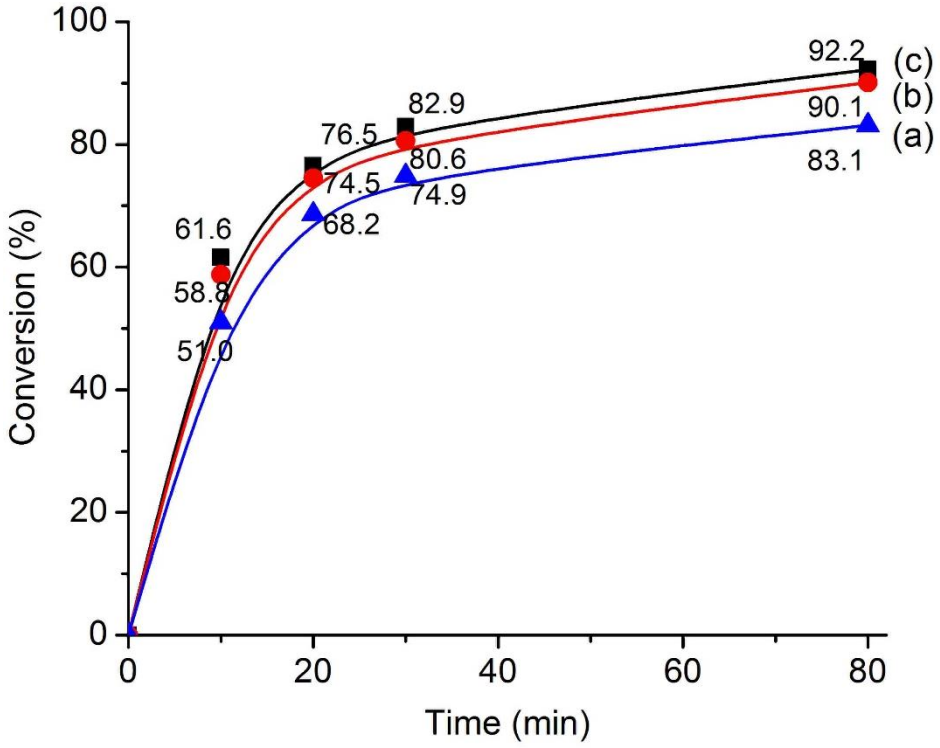

Fig. 8. Product conversion to vanillin acid catalyzed with (a) sodium hydroxide, (b) potassium hydroxide and (c) nanosized Cs-pollucite zeolite.

Catalyst reusability is a major problem in solid catalyst [47]. Hence, catalyst reusability is tested on nanosized Cs-pollucite. The catalytic activity of the recycled nanozeolite catalyst is preserved even after the fifth consecutive reaction cycle thanks to the strong bonding between the Cs^+ cations and the zeolite surface *via* electrostatic attraction forces (Fig. 9) [33]. The XRD pattern nanocrystalline Cs-pollucite zeolite after fifth cycle of catalytic reaction was obtained (Figure 10). The XRD peaks corresponding to ANA crystalline phase remain intact and no significant loss in crystallinity is shown. Thus, it reveals that the ANA crystalline framework structure of Cs-pollucite is stable even after multiple cycles of catalytic reaction. The XRD observation is further

supported by TEM and FESEM analysis (Fig. 11). As can be seen, the Cs-pollucite nanocrystals retain their morphology and shape while no interparticle nor intraparticle amorphization is shown in the TEM image confirming the highly crystalline nature of recycled Cs-pollucite nanocatalyst. Hence, the results suggest that nanosized Cs-pollucite zeolite can be used as a potential solid base catalyst besides other advanced applications.

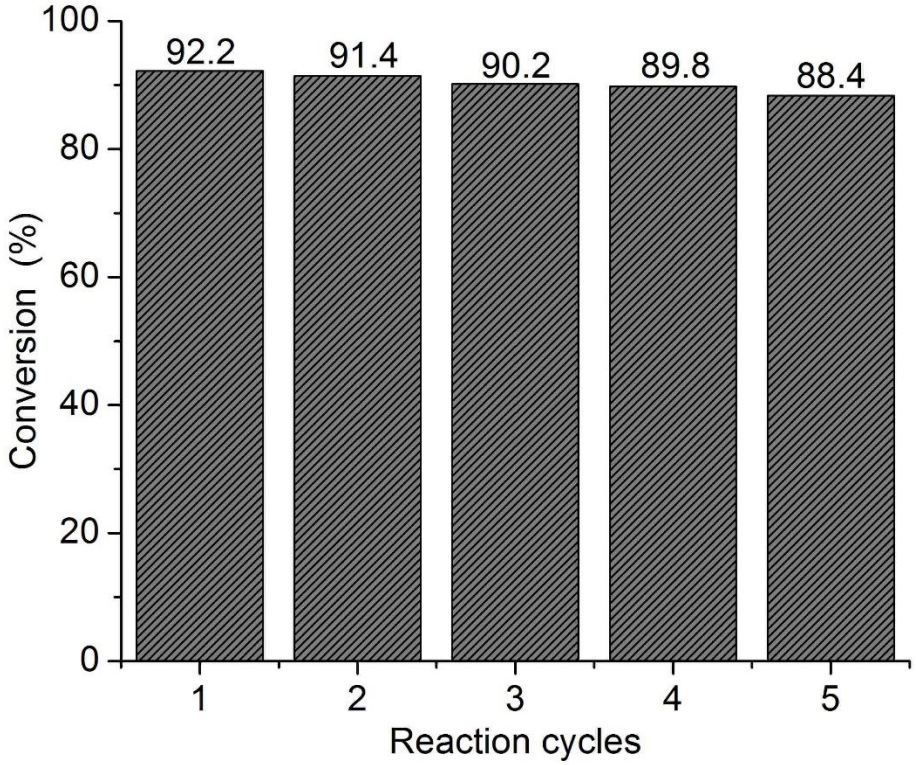

Fig. 9. Catalyst recycling test of nanosized Cs-pollucite zeolite in Perkin condensation reaction.

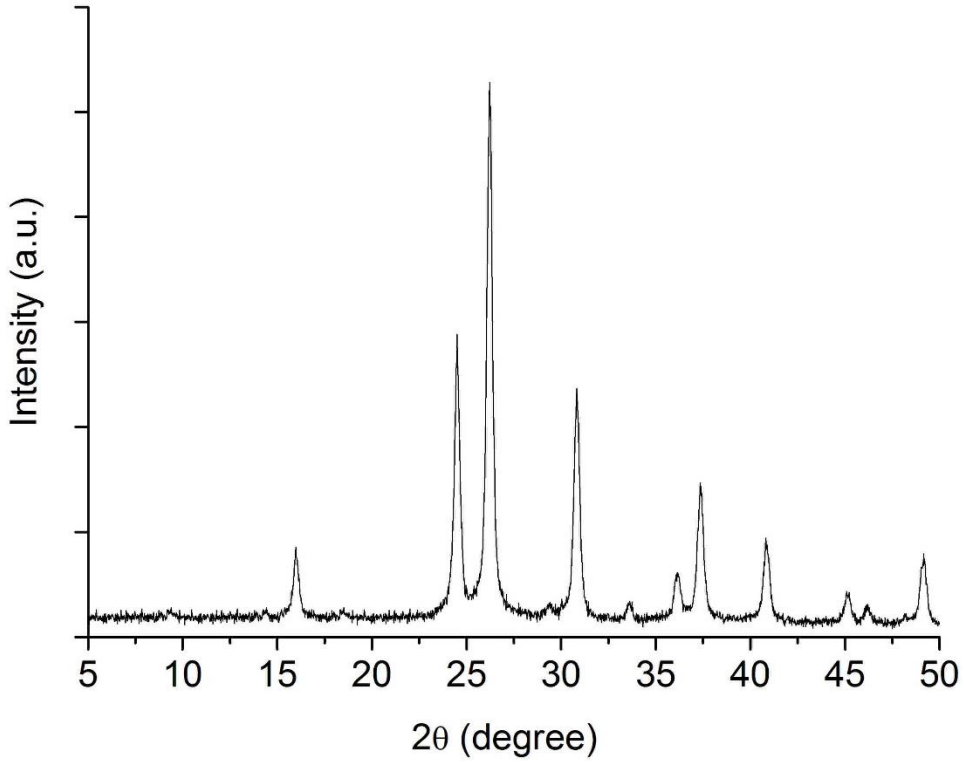

Fig. 10. XRD pattern of nanosized Cs-pollucite zeolite after 5 cycles of Perkin condensation reaction.

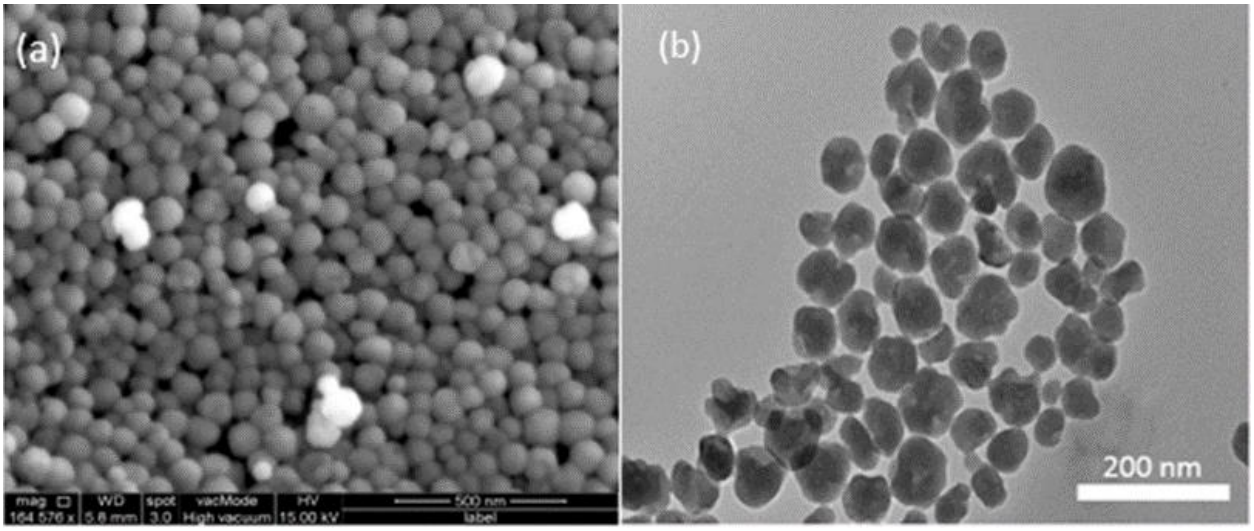

Fig. 11. (a) SEM and (b) TEM images of nanosized Cs-pollucite zeolite after recycling test.

4. Conclusion

One-pot hydrothermal synthesis of nanocrystalline Cs-pollucite zeolite (ca. 79.4 nm) *via* organotemplate-free approach is reported. The ANA framework (Si/Al ratio = 4.11) can be crystallized from a clear precursor within 50 h at mild temperature (180 °C). The Cs-pollucite dispersion is colloidally stable and is active in Perkin condensation of benzaldehyde with acetic anhydride. Thus, these nanocrystals with accessible mesoporosity have great potential in advanced applications particularly in film deposition and catalytic technologies.

Acknowledgement

The financial support from RUI (1001/PKIMIA/8011012) and SATU Joint Research Scheme (RU018O-2016) grants is gratefully acknowledged. The doctoral scholarship from University of Hail, Saudi Arabia is also acknowledged.

References

[1] M. Zhao, K. Deng, L. He, Y. Liu, G. Li, H. Zhao, Z. Tang, J. Am. Chem. Soc. 136 (2014) 1738-1741.

[2] M. Zhao, K. Yuan, Y. Wang, G. Li, J. Guo, L. Gu, W. Hu, H. Zhao, Z. Tang, Nature 539 (2016) 76-80.

[3] R. Weissleder, M. Nahrendorf, M.J. Pittet, Nat. Mater. 13 (2014) 125-138.

[4] T. Li, Z. Ma, F. Krumeich, A.J. Knorpp, A.B. Pinar, J.A. van Bokhoven, ChemNanoMat 4 (2018) 992-999

[5] X. Guo, L. Wu, D.R. Corbin, A. Navrotsky, Micropor. Mesopor. Mater. 274 (2019) 373-378.

[6] D.Y. Khoo, W.M. Kok, R.R. Mukti, S. Mintova, E.-P. Ng Solid State Sci. 25 (2013) 63-69.

[7] M.E. Davis, Nature 417 (2002) 813.

[8] V. Valtchev, L. Tosheva, Chem. Rev. 113 (2013) 6734-6760.

[9] E.-P. Ng, H. Awala, J.-P. Ghoy, A. Vincente, T.C. Ling, Y.H. Ng, S. Mintova, F. Adam, Mater. Chem. Phys. 159 (2015) 38-45.

[10] V. Valtchev, L. Tosheva, Chem. Rev. 113 (2013) 6734-6760.

[11] E.-P. Ng, L. Delmotte, S. Mintova, ChemSusChem. 2 (2009) 255-260.

[12] Y. Kamimura, W. Chailittisilp, K. Itabashi, A. Shimojima, T. Okubo, Chem. Asian J. 5 (2010) 2182-2191.

[13] S.-F. Wong, K. Deekamwong, J. Wittayakun, T.C. Ling, O. Muraza, H.L. Lee, F. Adam, E.-P. Ng, Sains Malaysiana 47 (2018) 337-345.

[14] H. Awala, J.P. Gilson, R. Retoux, P. Boullay, J.M. Goupil, V. Valtchev, S. Mintova, Nat. Mater. 14 (2015) 447-451.

[15] V.P. Valtchev, K.N. Bozhilov, J. Phys. Chem. B 108 (2004) 15587-15598.

[16] J. Kecht, B. Mihailova, K. Karaghiosoff, S. Mintova, T. Bein, Langmuir 20 (2004) 5271–5276.

[17] V.P. Valtchev, L. Tosheva, K.N. Bozhilov, Langmuir 21 (2005) 10724-10729.

[18] E.-P. Ng, G.K. Lim, G.-L. Khoo, K.-H. Tan, B.S. Ooi, F. Adam, T.C. Ling, K.-L. Wong, Mater. Chem. Phys. 155 (2015) 30-35.

[19] M. Tsapatsis, T. Okubo, M. Lovallo, M.E. Davis, Mat. Res. Soc. Symp. Proc. 371 (1995) 21-26.

[20] Y. Liu, M. Sun, C.M. Lew, J. Wang, Y. Yan, Adv. Funct. Mater. 18 (2008) 1732-1738.

[21] Y.-W. Cheong, K.-L. Wong, T.C. Ling, E.-P. Ng, Mater. Express 8 (2018) 463-468.

[22] K. Jiao, X. Xu, Z. Lv, J. Song, M. He, H. Gies, Micropor. Mesopor. Mater. 225 (2016) 98-104.

[23] T. Kurniawan, O. Muraza, K. Miyake, A.S. Hakeem, Y. Hirota, A.M. Al-Amer, N. Nishiyama, Ind. Eng. Chem. Res. 56 (2017) 4258-4266.

[24] W. Fan, K. Morozumi, R. Kimura, T. Yokoi, T. Okubo, Langmuir 24 (2008) 6952-6958.

[25] E.-P. Ng, L. Delmotte, S. Mintova, Green Chem. 10 (2008) 1043-1048.

[26] E.-P. Ng, K.-L. Wong, D.T.-L. Ng, H. Awala, R.R. Mukti, F. Adam, S. Mintova, Mater. Chem. Phys. 188 (2017) 49-57.

[27] G. Majano, K. Raltchev, A. Vicente, S. Mintova, Nanoscale 7 (2015) 5787-5793.

[28] X. Chen, D. Xi, Q. Sun, N. Wang, Z. Dai, D. Fan, V. Valtchev, J. Yu, Micropor. Mesopor. Mater. 234 (2016) 401-408.

[29] S. Mintova, J. Grand, V. Valtchev, Compt. Rend. Chim. 19 (2016) 183-191.

[30] G.D. Gatta, N. Rotiroti, T.B. Ballaran, C.S. -Valle, A. Pavese, Am. Mineral. 94 (2009) 1137-1143.

[31] L.M. Torres-Martinez, J.A. Gard, R.A. Howie, A.R. West, J. Solid State Chem. 51 (1984) 100-103.

[32] Y. Yokomori, K. Asazuki, N. Kamiya, Y. Yano, K. Akamatsu, T. Toda, A. Aruga, Y. Kaneo, S. Matsuoka, K. Nishi, S. Matsumoto, Sci. Rep. 4 (2014) 4195.

[33] Y. Chen, Z. Jing, K. Cai, J. Li, Chem. Eng. J. 336 (2018) 503-509.

[34] S. Mintova, N.H. Olson, T. Bein, Angew. Chem. Int. Ed. 38 (1999) 3201-3204.

[35] S.-F. Wong, H. Awala, A. Vincente, R. Retoux, T.C. Ling, S. Mintova, R.R. Mukti, E.-P. Ng, Micropor. Mesopor. Mater. 249 (2017) 105-110.

[36] S.-F. Wong, K. Deekomwong, J. Wittayakun, T.C. Ling, O. Muraza, F. Adam, E.-P. Ng, Mater. Chem. Phys. 196 (2017) 295-301.

[37] C.A.R. Reyes, C. Williams, O.M.C. Alarcon, Mater. Res. 16 (2013) 424-438.

[38] Database of International Centre for Diffraction Data (ICDD). http://www.icdd.com/.

[39] S. Mintova, J.P. Gilson, V. Valtchev, Nanoscale 5 (2013) 6693-6703.

[40] G. Majano, E.-P. Ng, L. Lakiss, S. Mintova, Green Chem. 13 (2011) 2435-2440.

[41] E.-P. Ng, D.T.L. Ng, H. Awala, K.-L. Wong, S. Mintova, Mater. Lett. 132 (2014) 126-129.

[42] E.-P. Ng, J.-Y. Goh, T.C. Ling, R.R. Mukti, Nanoscale Res. Lett. 8 (2013) 120.

[43] I. Yanase, Y. Saito, H. Kobayashi, Ceram. Inter. 38 (2012) 811-815.

[44] M. Rahimi, E.-P. Ng, K. Bakhtiari, M. Vinciguerra, H.A. Ahmad, H. Awala, S. Mintova, M. Daghighi, F.B. Rostami, M. de Vries, M.M. Motazacker, M.P. Peppelenbosch, M. Mahmoudi, F. Rezaee, Sci. Rep. 5 (2015) 17259.

[45] S.-F. Wong, K. Deekomwong, J. Wittayakun, T.C. Ling, O. Muraza, F. Adam, E.-P. Ng, Mater. Chem. Phys. 196 (2017) 295-301.

[46] K. Yanagisawa, M. Nishioka, N. Yamasaki, J. Nuclear Sci. Technol. 24 (1987) 51-60.

[47] A. Golmohamadpour, B. Bahramian, A. Shafiee, L. Ma'mani, Mater. Chem. Phys. 218 (2018) 326-335.